The A-Star Puzzle
Proceedings IAU Symposium No. 224, 2004
J. Zverko, J. Žižňovský, S.J. Adelman, & W.W. Weiss, eds.

DOI: 10.1017/S1743921304004430

Magnetorotational instability in Ap star envelopes

Reiner Arlt
Astrophysikalisches Institut Potsdam, An der Sternwarte 16, D-14482 Potsdam, Germany
email: rarlt@aip.de

Abstract. The rotational evolution of the radiative zone of magnetic Ap stars is investigated with numerical simulations. An angular-velocity profile decreasing with axis distance in combination with a magnetic field leads to a magnetorotational instability. The resulting flows efficiently transport angular momentum outwards. The corresponding decay of angular-velocity gradients in the radiative zone is estimated to take about 10–100 million years.

Keywords. MHD, instabilities, stars: rotation

1. The magnetorotational instability

Magnetic Ap stars rotate significantly slower than non-magnetic A stars. The Ap stars may either have magnetic fields because they are slow rotators, or they could rotate slowly because they possess magnetic fields. We are concerned with the latter of the two relations.

If the angular velocity of an object decreases with axis distance, the presence of a magnetic field causes an instability which will lead to flows reducing the gradient in angular speed. This local, linear instability was discovered by Velikhov (1959) in Taylor-Couette flows and was rediscovered and introduced to astrophysical flows by Balbus & Hawley (1991).

A few braking mechanisms acting on the star during its early life have been proposed such as magnetic star-disk locking and stellar winds. It is very important to note that these effects exert torques on the surface of the star and a coupling with the deeper layers of the star is needed to brake the entire interior. The microscopic viscosity in a radiative zone is much too small to provide an efficient coupling between the surface layers and the interior. This is why we have good reasons to assume that the interior of the star rotates faster than the surface.

The interesting fact about the magnetorotational instability (MRI) is that there is no lower limit for the magnetic field strength in ideal MHD. If there is a finite conductivity, there is of course a lower limit for the field strength, but since the microscopic conductivity of the stellar plasma in the radiative zone is extremely high, the lower limit for the MRI is below 1 G. As the magnetic field strength is decreased, the wavelength of the most unstable mode becomes shorter, too. The diffusive damping rate increases thereby. Since the diffusive decay and MRI growth will balance at a certain magnetic field strength, we consider this the minimum field strength. The minimum is plotted in Fig. 1 for various densities and differential rotations based on an A0 star. Various densities mean various loci in the star.

In the context of Ap stars, the upper limit will be more relevant. Again, a given magnetic field strength corresponds to a certain wavelength of perturbation which will grow the fastest. As the field strength is increased, this wavelength gets larger and may eventually exceed the size of the object, i.e., the stellar radius. The MRI will be much

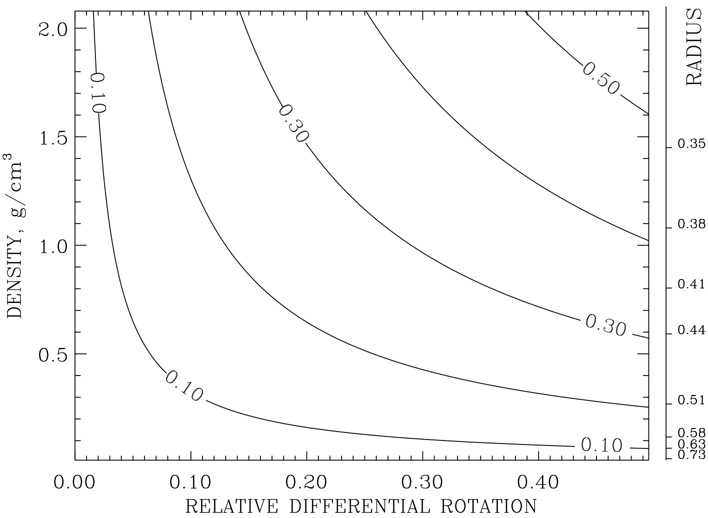

Figure 1. Minimum magnetic field strength in G for an A0 star envelope depending on differential rotation and density. At smaller field strengths, diffusion of the most unstable MRI mode will be faster than its growth rate in the nondiffusive case.

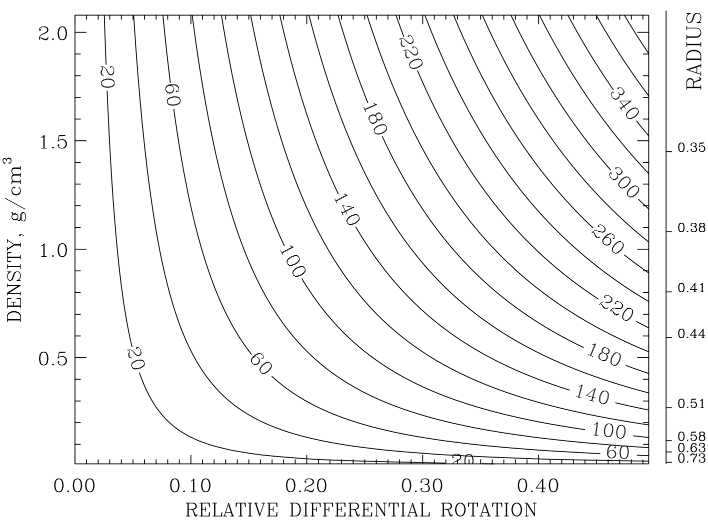

Figure 2. Maximum magnetic field strength in kG for an A0 star envelope depending on differential rotation and density. With stronger fields, the MRI will develop at highly reduced growth rates.

weaker beyond this field strength. We plotted this maximum field strength again for an A0 star as a function of differential rotation and density (or radius fraction) in Fig. 2. If the differential rotation is only about 10%, we can expect the MRI to occur up to field strengths of several tens of kG. Typically the surface fields of Ap stars do not exceed 3.5 kG (Bychkov *et al.* 2003). Assuming a dipole as the simplest field geometry, internal fields at $0.5R_*$ will then be 20–30 kG.

https://doi.org/10.1017/S1743921304004430 Published online by Cambridge University Press

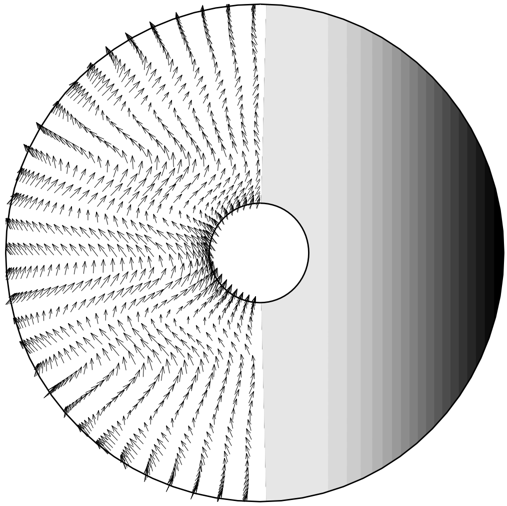

Figure 3. A vertical cross-section through the initial configuration with the magnetic field perturbation on the left side, and the angular velocity contours on the right side.

2. The numerical setup

A spherical, spectral numerical code developed by Hollerbach (2000) is applied to solve the MHD equations in the Boussinesq approximation,

$$\left(\frac{\partial}{\partial t} + \boldsymbol{u} \cdot \nabla\right)\boldsymbol{u} = -\nabla p + \mathrm{Pm}\nabla^2\boldsymbol{u} + (\nabla \times \boldsymbol{B}) \times \boldsymbol{B} \tag{2.1}$$

$$\frac{\partial \boldsymbol{B}}{\partial t} = \nabla^2\boldsymbol{B} + \nabla \times (\boldsymbol{u} \times \boldsymbol{B}) \tag{2.2}$$

with the usual meanings of $\boldsymbol{u}$, $\boldsymbol{B}$, and p as the velocity, magnetic field, and pressure which is not explicitly calculated in this model, but eliminated by applying the curl-operator to Eq. (2.1). Additionally, $\nabla \cdot \boldsymbol{u} = 0$ and $\nabla \cdot \boldsymbol{B} = 0$ hold, which are exactly preserved because potentials for velocity and magnetic field are used.

Normalizations are introduced using the outer radius R_*, the magnetic diffusivity η and an average density ρ, which lead to the non-dimensional quantities $\mathrm{Rm} = R_*^2\Omega_0/\eta$ – the magnetic Reynolds number, and $\mathrm{Pm} = \nu/\eta$ – the magnetic Prandtl number with ν being the kinematic viscosity. The normalized inner radius was $r_\mathrm{i} = 0.2$ and the outer radius was $r_\mathrm{o} = 1$.

The initial rotation profile depends on the axis distance, $s = r\sin\theta$ only. Such a profile fulfills the Taylor-Proudman theorem ensuring a minimum of purely hydrodynamic meridional circulations. The actual initial condition is

$$\Omega(s) = \frac{\mathrm{Rm}}{\sqrt{1 + (2s)^{2q}}}. \tag{2.3}$$

The exponent q is always set to 2; it will later be used as a fitting parameter to obtain a measure for the steepness of the rotation profile. The initial magnetic field is composed of a homogenous vertical field and a perturbation in a plane, with a wave vector parallel to the rotation axis,

$$\boldsymbol{B} = B_0[\hat{\boldsymbol{z}} + \epsilon\sin(kz + \pi/4)\hat{\boldsymbol{x}}], \tag{2.4}$$

where $\hat{\boldsymbol{z}}$ is the unit vector in the direction of the rotation axis and $\hat{\boldsymbol{x}}$ is a unit vector in

https://doi.org/10.1017/S1743921304004430 Published online by Cambridge University Press

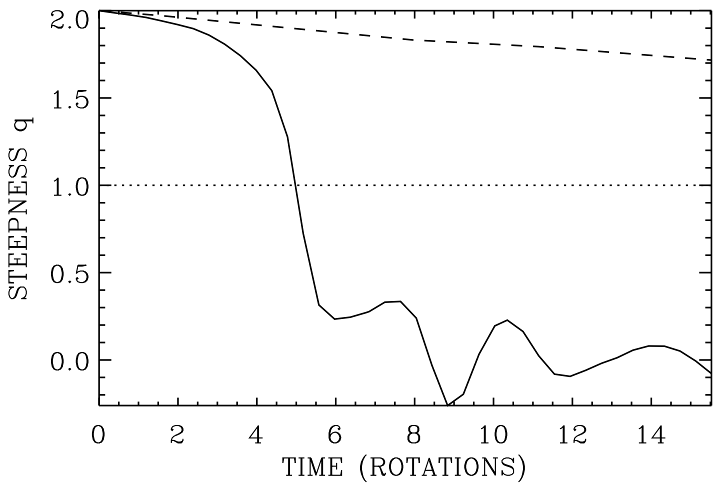

Figure 4. Decay of differential rotation measured by a steepness parameter q for $\mathrm{Rm} = 10^4$, taken from Arlt, Rüdiger & Hollerbach (2003). The dashed line is a hydrodynamic run for comparison.

the equatorial plane. The wave number of the perturbation is $k = 4\pi$. We added $\pi/4$ to the second term in (2.4) to provide mixed parity to the system. Equatorial and axial symmetry are thus broken allowing the nonlinear system to develop flows and fields in all modes. The initial configuration of magnetic field and angular velocity is shown in Fig. 3. The spectral truncation was set to 50 Chebyshev polynomials for the radial, 100 Legendre polynomials for the latitudinal and 30 Fourier modes for the azimuthal structure.

The MHD run quickly shows strong flows redistributing angular momentum in the radiative zone. Now we need a measure for the strength of differential rotation to evaluate the decay. The profile (2.3) is used with Rm and q now being free parameters. From each snap-shot of the simulation, we derive $\Omega(s)$ in the equatorial plane of the 'star'. This function is an average over all azimuths, since we are interested in the global rotation profile. A fit of (2.3) delivers a q for a number of time-steps. This steepness q is plotted versus time and shown in Fig. 4 for $\mathrm{Rm} = 10^4$. The dashed line shows the decay of differential rotation by pure viscosity. The decay time is much longer than the MHD decay. In a real star, the viscosity in the radiative zone is so small that the time-scale of viscous differential-rotation decay is of the order of 10^{13} yr.

Stellar Reynolds numbers are much larger than 10^4. Several runs were performed at various magnetic Reynolds numbers to get an extrapolated estimate for stellar conditions. As a result, the decay time amounts to roughly 10^7–10^8 yr. Since the age of the Sun is $5 \cdot 10^9$ yr, the process was fast enough to equalize differential rotation in the radiative core of the Sun. The more massive Ap stars have MS life-times of 10^9 yr or less. It is argued that the magnetorotational instability may be an ongoing process in the radiative envelopes of many of these stars.

Since radial motions will be strongly suppressed by buoyancy in radiative zones which are stably stratified, the simulation setup was improved by adding the effect of buoyancy. The MHD equations thus read

$$\left(\frac{\partial}{\partial t} + \boldsymbol{u} \cdot \nabla\right)\boldsymbol{u} = -\nabla p + \mathrm{Pm}\nabla^2\boldsymbol{u} + (\nabla \times \boldsymbol{B}) \times \boldsymbol{B} + \mathrm{Ra}_\eta \theta \boldsymbol{r} \tag{2.5}$$

https://doi.org/10.1017/S1743921304004430 Published online by Cambridge University Press

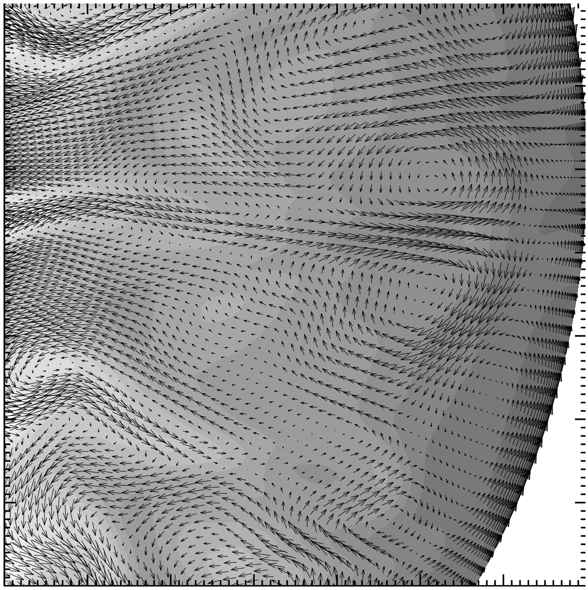

Figure 5. A vertical cross-section through part of the computational domain. The arrows are the meridional flow with the grey shading represents the angular velocity.

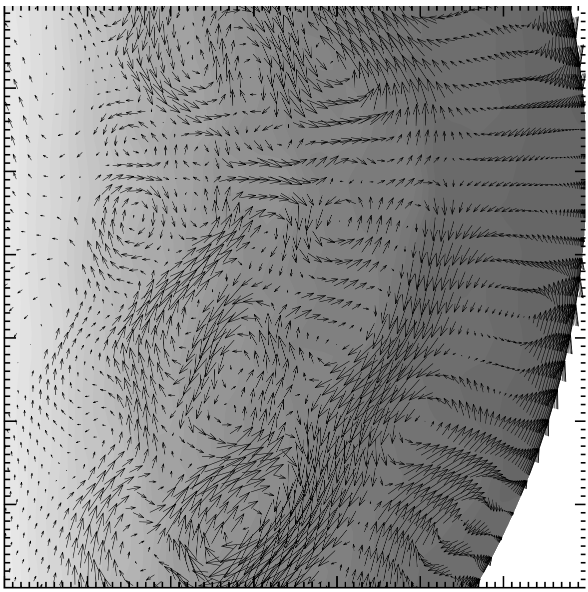

Figure 6. The same vertical cross-section as in Fig. 5, but including the stabilizing buoyancy force in the radiative zone.

$$\left(\frac{\partial}{\partial t} + \boldsymbol{u} \cdot \nabla\right)\theta = -u_r \frac{\partial T}{\partial r} + \frac{\mathrm{Pm}}{\mathrm{Pr}} \nabla^2 \theta, \tag{2.6}$$

with the unchanged induction equation (2.2). T and θ now denote an adiabatic background temperature profile and deviations from that, resp. Pr is the 'usual' Prandtl number defined by the viscosity and thermal diffusivity, ν/κ. The strength of the subadiabaticity is controlled by the dimensionless, modified Rayleigh number Ra_η which is based on the magnetic diffusivity rather than the viscosity.

https://doi.org/10.1017/S1743921304004430 Published online by Cambridge University Press

A cross-section through the velocity field at $\mathrm{Ra} = -10^8$ is shown in Fig. 6 at about the same time when the snap-shot in Fig. 5 was taken. Flows are much more horizontal. Yet, sufficient transport of angular momentum is found, leading to nearly the same decay time of 6 rotations (compared to 5 in the earlier model free of negative buoyancy). The angular-momentum transport will be highly suppressed at Rayleigh numbers $\mathrm{Ra} > 10^{10}$. Note again that these times from the numerical simulations will translate to much longer times using stellar parameters. Mixing in the outermost stellar layers by the MRI is less likely, because Ap star fields may exceed the maximum field there according to Fig. 2.

Acknowledgements

I am very grateful to R. Hollerbach for his help and making his MHD code available.

References

Arlt, R., Hollerbach, R. & Rüdiger, G. 2003, *A &A*, 401, 1087
Balbus S.A. & Hawley J.F. 1991, *ApJ*, 376, 214
Bychkov V.D., Bychkova L.V. & Madej J. 2003, *A &A*, 407, 631
Hollerbach, R. 2000, *Int. J. Numer. Meth. Fluids*, 32, 773
Velikhov, E.P 1959, *Sov. Phys. JETP*, 9, 995

Discussion

Moss: If this works to produce Ap stars as you suggest, why are not all A stars magnetic? A small seed-sized magnetic field could be expected to be present in any newly formed star. With any differential rotation (also likely to be present), the magnetorotational instability should be universal. Thus all A stars would be observably magnetic!

Arlt: The mechanism is not meant to *produce* Ap stars. Up to the moment when diffusion dominates the simulation, field amplifications of a factor of 10 are seen in the poloidal field. Starting with about 1 G, the resulting 10 G field will not easily be seen in A stars. Toroidal fields are amplified by a factor of $\sim$ Rm, but are hidden.

Stütz: To which extent do you think it is now possible to include more realistic microphysics and radiative transfe to get more realistic models?

Arlt: A full MHD simulation of a radiative envelope would require extensive radiative transfer computations at each MHD time-step. At present, these cannot be achieved in combination with the dynamics.

Noels: If the differential rotation is destroyed during the lifetime of an A star, is not there a danger to destroy the magnetic field at the same time? If this is the case, could it be that the field is smaller near the end of MS than at the ZAMS?

Arlt: The decay of differential rotation will have only a mediocre effect on the poloidal magnetic field which is observed. The magnetic field can actually be amplified using the differential rotation as an energy source. The following diffusive decay is very slow. Since the amplification of the (visible) poloidal field is weak, an observable evolutionary effect is not expected.

Mathys: The question of the evolution of the magnetic field during the MS lifetime has been looked into indeed: there is no evidence for a significant relation between the magnetic field intensity and the fraction of MS lifetime completed by the star.